

Wave run-up on a high-energy dissipative beach

Peter Ruggiero, R. A. Holman, R. A. Beach

Because of highly dissipative conditions and strong alongshore gradients in foreshore beach morphology, wave run-up data collected along the central Oregon coast during February 1996 stand in contrast to run-up data currently available in the literature. During a single data run lasting approximately 90 min, the significant vertical run-up elevation varied by a factor of 2 along the 1.6 km study site, ranging from 26 to 61% of the offshore significant wave height, and was found to be linearly dependent on the local foreshore beach slope that varied by a factor of 5. Run-up motions on this high-energy dissipative beach were dominated by infragravity (low frequency) energy with peak periods of approximately 230 s. Incident band energy levels were 2.5 to 3 orders of magnitude lower than the low-frequency spectral peaks and typically 96% of the run-up variance was in the infragravity band. A broad region of the run-up spectra exhibited an f^{-4} roll off, typical of saturation, extending to frequencies lower than observed in previous studies. The run-up spectra were dependent on beach slope with spectra for steeper foreshore slopes shifted toward higher frequencies than spectra for shallower foreshore slopes. At infragravity frequencies, run-up motions were coherent over alongshore length scales in excess of 1 km, significantly greater than decorrelation length scales on moderate to reflective beaches.

1. Introduction

The swash zone is the boundary between inner surf zone and subaerial beach processes and a significant amount of the total surf zone sediment transport occurs within this region [Osborne and Rooker, 1999]. Swash zone hydrodynamics govern swash zone sediment transport [Beach and Sternberg, 1991], are of considerable importance in determining the susceptibility of coastal properties to wave induced erosion [Ruggiero et al., 1996; Sallenger, 2000; Ruggiero et al., 2001], and play a critical role in the design and maintenance of shore protection structures [e.g., van der Meer and Stam, 1992]. Despite this importance, recent reviews

of swash zone processes [e.g., Elfrink and Baldock, 2002; Butt and Russell, 2000] highlight the lack of sufficient knowledge within this region.

Wave run-up, defined as the time-varying location of the shoreward edge of water on the beach face, is often expressed in terms of a vertical excursion consisting of two components: a super elevation of the mean water level, wave setup, and fluctuations about that mean, swash. Field investigations of run-up dynamics have typically taken place on intermediate to reflective beaches [e.g., Holman and Sallenger, 1985; Holman, 1986; Holland, 1995; Holland and Holman, 1999] and low energy and mildly dissipative beaches [e.g., Guza and Thornton, 1982; Raubenheimer et al., 1995; Raubenheimer and Guza, 1996] with the notable exception of the work of Ruessink et al. [1998], who examined run-up under highly dissipative conditions at Terschelling, Netherlands. On the basis of both laboratory observations of monochromatic waves [Hunt, 1959], and these extensive field observations, wave run-up is typically parameterized by

$$\frac{R}{H_s} = c\xi_o, \quad (1)$$

where R is a vertical run-up statistic (e.g., significant run-up height) normalized by H_s , the deep water significant wave height, c is a dimensionless constant, and ξ_o is the Iribarren number. The Iribarren number is a nondimensional “surf similarity” parameter that is useful in parameterizing a number of surf zone processes [Iribarren and Nogales, 1949; Battjes, 1974], and is given by

$$\xi_o = \frac{\tan \beta}{(H_s/L_o)^{1/2}}, \quad (2)$$

where β is the beach slope (assumed small, so that $\tan \beta \approx \sin \beta \approx \beta$), L_o is the deep water wave length given as $L_o = gT^2/2\pi$ by linear theory, g is the acceleration due to gravity, and T is the peak incident wave period. Low Iribarren numbers typically indicate dissipative conditions, while higher values suggest more reflective surf zones.

Through nonlinear interactions, incident band wave energy is transferred to both higher and lower frequencies through the surf zone [Longuet-Higgins and Stewart, 1962]. On dissipative beaches, infragravity energy (with frequencies roughly between 0.05 and 0.004 Hz) tends to dominate the inner surf zone, especially the swash zone. In contrast to the linear dependence of R/H_s on x_o given in equation (1), Guza and Thornton [1982] found that on relatively low energy dissipative beaches the infragravity component of R , which we shall refer to as R_{ig} , instead varied linearly with the offshore wave height only while the sea swell component, R_{ss} , remained constant. When analyzing a dissipative subset (low Iribarren numbers) of their data, Holman and Sallenger [1985] also showed this difference in behavior between the infragravity and incident bands of run-up. Ruessink et al. [1998] agreed, however they found the constant of proportionality between R_{ig} and H_s in equation (1) to be considerably higher on beaches with low Iribarren numbers.

Miche [1951] hypothesized that monochromatic incident waves can be thought of as having both a progressive and a standing component, and that the amplitude of swash oscillations is proportional to the amount of shoreline reflection and thus proportional to the standing wave amplitude. The standing wave amplitude at the shoreline reaches a maxima with waves just large

enough to be breaking, and therefore can be termed saturated as a further increase in wave height simply increases the amplitude of the progressive component which dissipates through wave breaking and has zero shoreline amplitude. Saturation therefore implies that the incident band swash amplitude does not increase with increasing offshore wave height, consistent with the aforementioned incident band results of Guza and Thornton [1982]. Qualitatively, Miche's hypothesis has been confirmed in the laboratory [Battjes, 1974; Guza and Bowen, 1976], in the field [Huntley et al., 1977; Guza and Thornton, 1982; Guza et al., 1984] and in the application of a numerical model based on the one-dimensional depth-averaged nonlinear shallow water equations [Raubenheimer et al., 1995; Raubenheimer and Guza, 1996].

Carrier and Greenspan [1958] analytically solved the nonlinear inviscid, shallow water wave equations on a planar beach and showed that a monochromatic, nonbreaking standing wave solution exists when

$$\varepsilon_s = \frac{a_s \omega^2}{g \tan^2 \beta} \leq 1, \quad (3)$$

where ε_s is another similarity parameter (high values indicate dissipative beaches) in which a_s is the vertical swash amplitude at the shoreline and ω is the wave angular frequency. Wave breaking initiates at $\varepsilon_s \approx 1.0$, and the swash amplitude at the shoreline has been shown to continue to increase until it reaches a saturation (critical) value ε_s^c . Estimates of this critical value range from 1.25 [Guza and Thornton, 1982] to 3.0 ± 1.0 [Guza and Bowen, 1976]. By combining Miche's [1951] hypothesis with equation (3) the normalized vertical run-up excursion [Stoker, 1947; Meyer and Taylor, 1972; Guza et al., 1984] becomes

$$\frac{R}{H_s} = \begin{cases} \left(\frac{\pi}{2\beta}\right)^{1/2} & : \xi_o \geq \xi_c : \text{reflective} \\ \frac{\xi_o^2}{\pi} & : \xi_o < \xi_c : \text{saturated} \end{cases}$$

(4)

where $\xi_c = (\pi^3/2\beta)^{1/4}$. Note that in the saturated region of equation (4), the dimensional form of R is independent of the wave height and has a β^2 dependence

$$R = \frac{\beta^2 L_o}{\pi} : \xi_o < \xi_c \quad (5)$$

as shown in equation (5) rather than the linear relationship with beach slope predicted by equation (1).

In analogy to the above monochromatic relationships, Huntley et al. [1977] suggested that for broadband swash, incident band frequencies in the vertical run-up energy density spectrum would become saturated and have the form

$$E(f) = \alpha f^4, \quad (6)$$

where α is a dimensional constant. Huntley et al. [1977] presented field results showing an f^4 spectral decay within this band, and by combining equation (3) with equation (5) suggested a “universal” form for the run-up spectrum

$$E(f) = [e_s^{c*} g \beta^2 / (2\pi f)^2]^2$$

where e_s^{c*} is now a dimensional constant related to the bandwidth of the saturated spectrum. Run-up energy densities in the saturated band are independent of offshore wave conditions as wave breaking prevents the magnitude of swash oscillations in the

saturated band from increasing past a certain level that depends on the beach slope squared. Guza and Thornton [1982] and Ruessink et al. [1998] showed similar saturated spectra from field data but with an f^{-3} roll off. Raubenheimer and Guza [1996] presented more run-up data with incident band saturation and their field observations, as well as results from the numerical model RBREAK [Kobayashi et al., 1989], both show an f^{-4} roll off.

The work presented in this paper extends analyses of run-up elevation time series to the high-energy and highly dissipative beaches common in the U.S. Pacific Northwest. While the only previous investigation into run-up dynamics under dissipative conditions presented alongshore averaged results [Ruessink et al., 1998], this study was designed to examine the variability of wave run-up statistics, spectral response, and alongshore structure over a 1.6 km alongshore distance on Agate Beach, Oregon. Our experimental design isolated the effects of strong alongshore gradients in foreshore beach morphology on wave run-up. The methodology of obtaining the video derived run-up data is described in section 2, and results can be found in section 3. The universality of equation (7) can be tested with a strongly alongshore variable beach slope, a condition met in our experiment and discussed in section 4. In section 4 we also compare and contrast the results of this study (and other similar studies on the dissipative Oregon coast) with those of Ruessink et al. [1998]. Finally, conclusions are summarized in section 5.

2. Methods

Run-up data were obtained during the High Energy Beach Experiment at Agate Beach in Newport, Oregon, during February 1996 as one component of an investigation into the dynamics of high-energy dissipative beaches. It is not uncommon for these low sloping, meso-tidal, and fine-grained (median grain-size diameter of 0.2 mm) beaches to experience winter deep water significant wave heights in excess of 8.0 m [Tillotsen and Komar, 1997; Allan and Komar, 2002]. Agate Beach, Oregon is dissimilar to the majority of previous run-up investigations, as large amplitude,

low-frequency motions are the dominant forcing within the inner to middle surf zone [Holman and Bowen, 1984; Ruggiero et al., 2001].

The field experiment was designed to characterize the temporal and spatial scales of low-frequency run-up motions and their potential role in suspended sediment transport. In situ instrumentation, consisting of current meters, suspended sediment sensors and pressure sensors, were deployed in the inner surf zone in a cross-shaped pattern with cross-shore and alongshore arrays of approximately 120 x 320 m. Video monitoring of wave breaking intensity, as well as detailed surveys of the foreshore, were also performed.

The experiment lasted for 11 days, from 7 February to 17 February 1996, during which the deep water significant wave height ranged from 1.4 to 4.1 m, peak wave periods ranged from 5 to 17 s, and the mixed semi-diurnal tide typically had a 2 to 3 m vertical excursion. The wave height and period data were obtained from the Coastal Data Information Program (CDIP) buoy offshore from Bandon, Oregon located in approximately 64 m of water, 100 km to the south of the study site. During the experiment the wave heights from the CDIP buoy compared well with data from the microseismometer system operated by Oregon State University at the Marine Science Center in Newport, Oregon, as well as the (National Data Buoy Center, NDBC) deep water buoy offshore from Newport. Although the latter two data sources are closer to the experiment site, the microseismometer typically provides a poor estimate of wave periods and the NDBC buoy has been found to over predict large wave heights by approximately 10% [Tillotsen and Komar, 1997]. Tide data were taken from the NOAA/ NOS tide gage No. 9435380 in Yaquina Bay Newport, Oregon, located approximately 6 km from the study site.

Figure 1 shows an oblique (Figure 1a) and plan (Figure 1b) view of 10-min time-averaged video exposures taken at Agate Beach at low tide on 11 February 1996, with the Agate Beach Argus cameras, a remote video system located on Yaquina Head that has

been operational since 1992. Regions of higher image intensity result from waves breaking preferentially over shallow bathymetric features [Lippmann and Holman, 1989]. The plan view, with the positive cross-shore direction being offshore and positive alongshore direction being to the south, reveals three, and in some areas four, sandbars offshore of the study area. The pluses indicate the locations of the in situ instrumentation deployed during the experiment.

Video recordings of run-up were made using three temporary video cameras mounted on Yaquina Head (near the long-term Argus camera), a basalt promontory located approximately 2 km to the north of the in situ instrumentation (alongshore distance $y \sim 2000$ m, not shown in Figure 1). Overlap in the field of view of the three cameras allowed for continuous coverage of the swash zone over an alongshore distance of approximately 1.6 km. The data discussed below consist of a single 1.5 hour Agate Beach wave run-up elevation time series measured along 33 individual cross-shore transects spaced every 50 m in the alongshore on 11 February 1996, from 1559 to 1729 LT. During this data run the swell dominated deep water significant wave height was 2.3 m, the wave period was 13 s, and the tide was high. Figure 2 is a snapshot from the camera aimed furthest north. Overlaid in the field of view are the cross-shore transects along which run-up was digitized, for this particular camera, extending from an alongshore position of $y = -1200$ m to $y = -950$ m. The middle camera covered the region extending from $y = -950$ m to $y = -350$ m, and the southerly looking camera extended the run-up coverage to $y = 400$ m.

Using the known geometric transformation between ground and image coordinates (via surveyed targets on the beach), the light intensity of each pixel in the cross-shore transects was digitized. Vertical run-up elevation time series were extracted from the video recordings using the “timestack” method [e.g., Aagaard and Holm, 1989; Holland and Holman, 1993, 1999]. The run-up position at each video sample time (1 Hz) is the landwardmost identifiable

edge of water determined via standard image processing algorithms along with substantial manual refinements. Holman and Guza [1984] and Holland et al. [1995] demonstrated that run-up extracted from video records roughly corresponds to data acquired with resistance wire run-up gauges supported less than a few centimeters above the beach face.

The vertical resolution of the video technique varies with both lens properties and distance from the cameras and is estimated by mapping the horizontal pixel resolution (typically <1.0 m) to an elevation along a cross-shore transect. Therefore, to extract run-up elevations along individual transects from video using the “timestack” technique, the topography of the beach is needed in addition to the geometry of the cameras. To obtain the beach surface topography over such large cross-shore and alongshore distances, Real Time Kinematic Differential Global Positioning System (RTK DGPS) surveying techniques were employed. A GPS receiver was installed on a six-wheeled amphibious vehicle that, by traveling approximately 5 m/s, yielded a dense mapping of the large beach surface in only a few hours with a vertical resolution on the order of 5 cm [Plant and Holman, 1997]. Figure 3 is a contour map of the intertidal and subaerial portion of Agate Beach from data obtained on 11 February 1996, at low tide. The definition of foreshore slope in this study is taken to be the best linear fit of the measured beach surface between \pm two standard deviations from the mean run-up elevation, a cross-shore distance typically greater than 100 m. Defined in this manner, the foreshore slope varied greatly in the alongshore, averaging approximately 0.014 over the experiment domain. Because of the low sloping beach, the vertical resolution of the run-up elevations derived from the video is taken to be 0.05 m, the survey accuracy, throughout the 1.6 km run-up transect array.

For subsequent analyses we separate the 1600 m run-up array into two regions based on differences in the foreshore beach slope (Figure 3). Region I, with a relatively steeper foreshore, consists of

both the northern, $y = -1200$ m to $y = -825$ m, and the southern, $y = -175$ m to $y = -400$ m, sections of the study area, while region II covers the middle section, $y = -825$ m to $y = -175$ m. Two typically low flowing drainages from the backing bluff had more substantial flows during the experiment due to heavy rainfall preceding the experiment. These flows deposited sediment in small deltas on the foreshore causing the extremely flat slopes in region II.

3. Results

Analysis of the 33 transectsofrun-up data during the single 1.5 hour Agate Beach data run on 11 February 1996 is separated into four categories; bulk statistics, frequency dependence, alongshore scale, and alongshore structure. Results for each category are summarized below.

3.1. Run-Up Statistics

During the 1.5 hour time series, the significant vertical run-up height, R , defined hereinafter as 4σ where σ^2 is the total variance of the run-up elevation time series at a particular transect, varied by more than a factor of 2 along the 1600 m study region. The alongshore variability of R (ranging from 0.6 to 1.4 m) obtained along 33 individual cross-shore transects, reveals a strong dependence on foreshore beach slope (cross-correlation coefficient of 0.85, Figure 4; correlations significantly different from zero with 95% confidence have absolute values greater than 0.34). A clear reduction in R is evident in region II, $y = -825$ to $y = -175$, where the average beach slope is a mild 0.009. The average slope in region I is 0.019 while the foreshore slope varies by a factor of 5 over the entire study area, ranging from 0.005 to 0.025.

The run-up data have been band partitioned to determine the sea swell (incident band) component ($0.05 \text{ Hz} < f < 0.2 \text{ Hz}$) and the infragravity band component ($f < 0.05 \text{ Hz}$) of R . On average, the infragravity band contained 96% of the total run-up variance, ranging from 91% to almost 100%, while the incident band was saturated. The ratio R_{ig}/R averaged 0.98 over the 33 transects suggesting a more highly dissipative field site than that of

Ruessink et al. [1998] who reported a data set averaged ratio of 0.85. A linear correlation between both R_{ig} and R_{ss} and the foreshore beach slope for this data run are significant at the 0.05 confidence level (not shown), $r = 0.83$ and 0.93 respectively. Both the ratio R_{ig}/R and the significant run-up period, T_{sw} (calculated using a zero down-crossing method in the time domain), at each transect decrease approximately linearly with increasing foreshore slope (Figure 5; $r = -0.86$ and $r = -0.90$, respectively).

3.2. Frequency Dependence

To illustrate the relative dominance of low-frequency energy on the highly dissipative Agate Beach study site we show an example 5-min run-up time series (sampled at 1 Hz) from the experiment (Figure 6). Time series from multiple cross-shore transects have been offset vertically to reveal structure in the alongshore (the data is spaced at 50 m). While the peak period during this data run was 13 s, the data reveal only a few discernible run-up maxima over the 5-min record. Individual wave crests can be followed over alongshore distances of well over 800 m at infragravity band frequencies (Figure 6).

Run-up energy density spectra were calculated from each quadratically detrended run-up elevation time series at the 33 cross-shore transects. Band averaging resulted in 18 degrees of freedom with a bandwidth of 0.0017 Hz. The most obvious feature in the spectra are the energy peaks at extremely low frequencies, approximately 0.0043 Hz for both regions I and II, peaks at lower frequencies than previously published run-up data (Figure 7). However, there is a clear division between spectra derived from region I, transects with steeper foreshore slopes, and spectra from the shallower sloping region II. Figure 7b displays averages of the run-up spectra from each region. Although the two spectra have energy peaks at similar low frequencies, the average spectrum from region I, has more energy at all higher frequencies than the spectrum from region II. There is a sharp roll off in energy beyond the peak frequencies,

and at the cutoff between the infragravity and incident bands, 0.05 Hz, the spectra have dropped 2.5 to 3.0 orders of magnitude in energy. The triangles in Figures 7a and 7b indicates the peak frequency of the incident deep water waves for this particular run (13 s wave period).

The average spectra reveal a saturated region, approximately proportional to f^4 , extending to lower frequencies than previously reported by most other researchers (Figure 7). Both Huntley et al. [1977] and Raubenheimer and Guza [1996], show saturated run-up spectra extending only throughout the incident band. Guza and Thornton [1982] show saturated run-up spectra, with an f^3 roll off rather than the f^4 dependence of the other studies (a result they thought to be due to differences in measurement techniques, wire run-up gages used in their study versus video used in others), extending into the infragravity band to approximately 0.04 Hz. The lowest saturated frequency, f_s , for the Oregon data, calculated using the technique described by Ruessink et al. [1998], ranges from approximately 0.0043 Hz to 0.0161 Hz with a mean of 0.01 Hz.

Figure 7b illustrates that the saturated portion of the spectra from region II, the region with the lower beach slopes, extends to slightly lower frequencies than in region I. Only the data of Ruessink et al. [1998] show saturation as deep into infragravity frequencies, however their data rolled off proportional to f^3 rather than the f^4 relationship shown here (even though they used video techniques to measure run-up). An f^3 spectral slope explains only 52% of the variance in the average spectra from each of the two regions in the 11 February 1996, Agate Beach data, while an f^4 spectral slope explains over 90% of the variance.

3.3. Alongshore Coherence Length Scales

Agate Beach, Oregon, is extremely dissipative, primarily due to its low foreshore slope. This, coupled with high-energy offshore wave conditions, results in large

morphodynamic and hydrodynamic cross-shore length scales with sandbars typically located up to several hundreds of meters from the shoreline (Figure 1) and winter storm waves that often break over 1 km offshore. These large cross-shore length scales and the low frequencies that dominate the inner surf zone suggest that the alongshore length scales of the system may also be quite large [Holman and Bowen, 1984]. Holland [1995] defined a simple measure of the alongshore structure of run-up motions as the length scale over which run-up motions of a given frequency are coherent. To determine the alongshore structure of the 11 February 1996, Agate Beach data run, squared coherence values were calculated from the cross-spectral matrix of all possible run-up sensor (run-up transects) pairs as a function of frequency and sensor separation (alongshore lag). An example is shown in Figure 8 in which the squared coherence has been calculated for the peak frequency (0.0043 Hz) from the average spectra in region I. The critical squared coherence level (95% significance) is calculated as a function of lag due to the variable number of corresponding realizations and increases with longer lags (fewer realizations). An alongshore coherence length scale, L_c , is defined as the maximum lag with a squared coherence level above the critical value, for which all shorter lags have squared coherence levels that are also significant. For the peak frequency of 0.043 Hz the coherence length scale is approximately 1250 m (Figure 8).

Characteristic alongshore length scales have been computed in this manner for all frequencies in the infragravity band and are shown in Figure 9. The Agate Beach run-up data is coherent over alongshore length scales ranging from 300 m to over 1000 m within the range of lowest saturated frequencies, f_s . These results are qualitatively consistent with observations of the time series shown in Figure 6 and replays of the video records. However, the

alongshore coherence length scales are approximately an order of magnitude longer than those found by Holland and Holman [1999] on a more moderate to reflective U.S east coast beach.

3.4. Wave Number-Frequency Structure

Potential mechanisms responsible for forcing the energetic motions found in the run-up data at very low infragravity frequencies include both the reflection of incoming waves and the nonlinear forcing of leaky and trapped edge wave modes by incident wave groups. Measurements of the alongshore variability of wave run-up provide alongshore phase relations that can be used to define an alongshore wave number, k_y . Using k_y , it can be determined if the infragravity energy is in the form of trapped or leaky edge waves [Holland and Holman, 1999]. For a particular angular frequency, ω , these possibilities are distinguished by

$$\begin{aligned}\omega^2 &\leq gk_y: \text{edge waves} \\ \omega^2 &\geq gk_y: \text{leaky modes}\end{aligned}\quad (8)$$

The wave number for which the equality holds is termed the cutoff mode. A wave number-frequency spectrum, derived from an iterative maximum likelihood estimator (IMLE) [Pawka, 1982], was calculated to investigate the dynamics of the run-up motions over the length of the video transect array (not shown). The majority of the energy was concentrated at extremely low wave numbers and there is no clear evidence of low mode edge waves. Because of the extremely low frequencies of the motions, the 1600 m array length becomes relatively short. For the peak frequency of the average run-up spectrum from section II (0.0043 Hz), the approximate cutoff wavelength separating the edge wave and leaky mode regimes is 84 km. Therefore we are unable to resolve the difference between leaky modes and higher edge wave modes.

4. Discussion

Guza and Thornton [1982] showed that for a particular beach slope, run-up spectra have approximately the same energy level in the saturated frequency range, regardless of incident wave conditions. The Huntley et al. [1977] dimensional proportionality, α , from equation (6), depends on the foreshore slope and determines what this energy level should be. This parameter, and the actual power of the roll off of the saturated run-up energy density spectrum, can be calculated by fitting spectral estimates within the saturated band to the form of equation (6) in log-log space. For the saturated portion of the average spectrum in region I, the top line in Figure 7b, the energy density spectrum has the form $E(f) = 1.2 \times 10^{-7} f^{4.14}$. The constant derived for the average spectrum in region II is approximately an order of magnitude less and the power dependence is f^4 . These relationships are shown in Figure 7b as the solid lines through the spectral estimates within the saturated band. The universal form for the saturated run-up spectrum suggested by Huntley et al. [1977], equation (7), requires α to be proportional to β^4 . To test this dependence, the constant α has been calculated for each of the 33 transects in our run-up array during the 11 February 1996 Agate Beach data run. Figure 10 shows the estimates from the Agate Beach data as well as data taken from Huntley et al. [1977]. The data of Huntley et al. [1977] is derived from four different beaches all with a much greater foreshore beach slope than Agate Beach. The best fit through the data in loglog space is shown as the solid line. The calculated power of the dependence between α and β including both data sets is 2.85 rather than 4.0 as suggested by equation (7). Using just the Agate Beach data the power of the dependence becomes 2.0, analogous to the linear relationship between the significant run-up elevation and beach slope shown in

Figure 4. The saturated sections of the average spectra from the two regions in the Agate Beach data are therefore separated by a constant proportional to β^2 (Figure 8) rather than β^4 .

The value of e_s^{c*} from equation (7), a dimensional constant with the nonphysical units of $\text{Hz}^{-1/2}$, can be determined from the estimates of α using the following relation

$$\epsilon_s^{c*} = \frac{\alpha^{1/2}(2\pi)^2}{g\beta^2}. \quad (9)$$

Note that if α is not proportional to β^4 , as in the case of the data presented in Figure 10, estimates of e_s^{c*} also must depend on the beach slope. From arguments of down slope swash accelerations, Huntley et al. [1977] define a nondimensional universal constant, $e_s^{c*}(\Delta f)^{1/2}$, approximately equal to 1.0, where Δf is taken as the bandwidth over which wave breaking is occurring. Therefore, for the data presented in this paper with constant wave conditions, the universal constant suggested by Huntley et al. [1977] is in fact not a constant but a function of the foreshore beach slope.

The linear dependence of R_{ig} on β for the single Agate Beach data run presented in this paper lends credibility to the typical linear parameterization of run-up with the foreshore slope, defined as in equation (1) or in a similar fashion. However, these results stand in contrast to the β^2 relationship predicted for saturated run-up by equation (5) and the results of Raubenheimer and Guza [1996]. More significantly, these results contrast with the lack of any significant relationship between R_{ig} and β found by Ruessink et al. [1998] on a dissipative beach in Terschelling,

Netherlands. Ruessink et al. [1998] also noted a lack of a significant relationship between T_{sw} and β (as found in this study, Figure 5), a result they related to the limited range of β values in their data set. Another possibility for these differences is the alongshore averaging performed by Ruessink et al. [1998], and not performed here, that potentially masks subtle influences of the alongshore variability of β on run-up. Further, only during a single video run, when deep water wave conditions are constant, can the effect of β on run-up be completely isolated.

While the results presented thus far were obtained from only a single Agate Beach data run, Figures 11 through 13 feature additional run-up data derived from dissipative Oregon beaches. These data, obtained from other runs analyzed during the 1996 Agate Beach experiment, as well as from earlier run-up experiments between 1991 and 1995, total 74 individual run-up time series. These data were obtained utilizing video techniques and are described in detail by Ruggiero et al. [1996, 2001]. This complete Oregon run-up data set has also been band partitioned with the infragravity band containing an average of 96% of the total run-up variance, ranging from 77% to 99% (STD = 0.05). Again, the incident band is typically fully saturated. A linear correlation between R_{ig} and the foreshore slope for all of the Oregon data is now only weakly significant at the 0.05 confidence level (Figure 11), $r = 0.34$, while a linear relationship between the sea swell component and slope is highly significant, $r = 0.92$. These results, when including all of the Oregon run-up data, more closely agree with the results of Ruessink et al. [1998] as the direct effect of beach slope on run-up is potentially masked by the inclusion of multiple data runs with varying offshore wave conditions. The frequency band-partitioned significant run-up for all of the Oregon data is plotted versus wave height in

Figure 12, with the pluses representing the incident band and the circles representing the infragravity band. In order not to overly weigh the results from the 33 transects during the single 11 February 1996, Agate Beach data run discussed above, only an alongshore average for each (beach slope) region has been included. The best linear fit through the infragravity band of all of the Oregon run-up data gives the statistically significant relationship

$$R_{ig} = 0.33H_s + 0.33; r = 0.67. \quad (10)$$

These results are consistent with a saturated incident band, however, the Oregon run-up values are consistently higher than those predicted by Ruessink et al. [1998], $R_{ig} = 0.18 H_s + 0.16$. The constant of proportionality, 0.33, in the linear fit relating R_{ig} and H_s , is nearly twice as large as the 0.18 found by Ruessink et al. [1998] for dissipative beaches but is much smaller than the 0.7 found by Guza and Thornton [1982].

[31] All of the Oregon run-up data fall within a relatively small dissipative range of Iribarren numbers, $\xi_o < 0.5$, (Figure 13) and reveal no statistically significant dependence of normalized significant run-up height on this parameter. However, the range of ξ_o may be large enough to lend support to the observation of Ruessink et al. [1998], that the dependence of R_{ig}/H_s on ξ_o appears to change near a value of approximately 0.3. To demonstrate this, we show the full Oregon data set along with relationships derived by Ruessink et al. [1998], Holman and Sallenger [1985], and Holland [1995]. While the Ruessink et al. [1998] relationships are derived from a dissipative beach; the latter two relationships are derived from a moderate to reflective beach in Duck, North Carolina. The correlation between the Oregon data and the Iribarren number is significant at the 0.05 confidence level for Iribarren numbers less than approximately 0.3. Similar to the observation of Ruessink et

al. [1998], the slope of the regression is steeper for smaller Iribarren numbers than for Iribarren numbers greater than 0.3. However the difference in slopes across this Iribarren number threshold is less for the Oregon data, which have a slope of 1.1, for $\xi_o < 0.3$, as compared to the 2.2 shown by Ruessink et al. [1998]. The slope of the relationship between R_{ig}/H_s on ξ_o (weakly significant at the 0.05 confidence level using only 9 points), for $\xi_o > 0.3$, is 0.7 for the Oregon data, relatively similar to the 0.5 value in each of the relationships derived at Duck. Ruessink et al. [1998] suggest that the steeper relationship between R_{ig}/H_s and ξ_o on highly dissipative beaches is due to the downshift of the extent of saturation into the infragravity band, another result supported by the Oregon data.

5. Conclusions

Wave run-up data derived from video recordings on a U.S. Pacific Northwest beach are dominated by infragravity energy with spectral peaks at approximately 0.0043 Hz. This behavior, on a strongly dissipative beach, contrasts with the majority of run-up data collected on more moderate beaches that are dominated by incident band energy. All calculated run-up spectra show a broad saturated region with an f^{-4} dependence extending deeper inside the infragravity frequency band than previously reported. Run-up motions at peak infragravity frequencies were coherent over large alongshore length scales, on the order of 1 km. The cutoff wave length for leaky modes is approximately 84 km at the peak run-up frequencies, so even with a 1.6 km data array most edge wave modes were underresolved. The extension of the universal form for shoreline run-up spectra of Huntley et al. [1977] to extremely low sloping beaches indicates an unpredicted dependence on beach slope.

Significant wave run-up height, collected during a single 1.5 hour February 1996 data run along a 1.6 km

highly dissipative stretch of coast, demonstrates a clear dependence on the local foreshore beach slope. This dependence is most likely due to the strong measured alongshore gradients in foreshore beach morphology coupled with the alongshore-constant wave conditions during the single data run, conditions not met in earlier run-up experiments.

However, when examining all data runs on high-energy dissipative Oregon beaches (74 individual time series over a range of wave conditions) the relationship between R and β becomes relatively weak, more closely agreeing with the results of the only previously published run-up data on dissipative beaches [Ruessink et al., 1998]. While the Oregon run-up data discussed in this paper lend qualified support to the Ruessink et al. [1998] assertion that different relationships between R_{ig}/H_s and ξ_o exist for $\xi_o > 0.3$, more investigation into this possible transition zone in Iribarren number space is clearly warranted.

Acknowledgments. The High Energy Beach Experiment was supported by the ONR Coastal Dynamics program under grant N000-14-94-11196. A portion of the manuscript was written while the U.S. Geological Survey's Mendenhall Postdoctoral Program supported P. R. We would like to thank those at the Coastal Imaging Lab of OSU who participated in the field experiment as well as Dan Hanes, Hilary F. Stockdon, and two anonymous reviewers for providing detailed reviews of an earlier form of this manuscript.

References

- Aagard, T., and D. Holm (1989), Digitization of wave runup using video records, *J. Coastal Res.*, 5, 547–551.
- Allan, J. C., and P. D. Komar (2002), Extreme storms in the Pacific Northwest coast during the 1997–98 El Niño and 1998–99 La Niña, *J. Coastal Res.*, 18, 175–193.

- Battjes, J. A. (1974), Surf similarity, paper presented at the 14th Coastal Engineering Conference, Am. Soc. of Civ. Eng., Copenhagen, Denmark.
- Beach, R. A., and R. W. Sternberg (1991), Infragravity driven suspended sediment transport in the swash, inner and outer-surf zones, in Coastal Sediments '91, pp. 114– 128, Soc. of Civ. Eng., New York, N. Y.
- Butt, T., and P. Russell (2000), Hydrodynamics and cross-shore sediment transport in the swash zone of natural beaches: A review, J. Coastal Res., 16, 255– 268.
- Carrier, G. F., and H. P. Greenspan (1958), Water waves of finite amplitude on a sloping beach, J. Fluid Mech., 4, 97– 109.
- Elfrink, B., and T. Baldock (2002), Hydrodynamics and sediment transport in the swash zone: A review and perspectives, Coastal Eng., 45, 149–167.
- Guza, R. T., and A. J. Bowen (1976), Resonant interactions for waves breaking on a beach, paper presented at 15th Coastal Engineering Conference, Am. Soc. of Civ. Eng., Honolulu, Hawaii.
- Guza, R. T., and E. B. Thornton (1982), Swash oscillations on a natural beach, J. Geophys. Res., 87, 483– 491.
- Guza, R. T., E. B. Thornton, and R. A. Holman (1984), Swash on steep and shallow beaches, paper presented at 19th Coastal Engineering Conference, Am. Soc. of Civ. Eng., Houston, Tex.
- Holland, K. T. (1995), Foreshore dynamics: Swash motions and topographic interactions on natural beaches, Ph.D. thesis, Oreg. State Univ., Corvallis, Oreg.
- Holland, K. T., and R. A. Holman (1993), The statistical distribution of swash maxima on natural beaches, J. Geophys. Res., 87, 10,271– 10,278.
- Holland, K. T., and R. A. Holman (1999), Wavenumber-frequency structure of infragravity swash motions, J. Geophys. Res., 104, 13,479– 13,488.

Holland, K. T., B. Raubenheimer, R. T. Guza, and R. A. Holman (1995), Runup kinematics on a natural beach, *J. Geophys. Res.*, 100, 4985– 4993.

Holman, R. A. (1986), Extreme value statistics for wave run-up on a natural beach, *Coastal Eng.*, 9, 527– 544.

Holman, R. A., and A. J. Bowen (1984), Longshore structure of infragravity wave motions, *J. Geophys. Res.*, 89, 6446– 6452.

Holman, R. A., and R. T. Guza (1984), Measuring runup on a natural beach, *Coastal Eng.*, 8, 129– 140.

Holman, R. A., and A. H. Sallenger (1985), Setup and swash on a natural beach, *J. Geophys. Res.*, 90, 945– 953.

Hunt, I. A. (1959), Design of seawalls and breakwaters, *J. Waterw. Harbors Coastal Eng. Div. Am. Soc. Civ. Eng.*, 85, 123– 152.

Huntley, D., R. T. Guza, and A. J. Bowen (1977), A universal form for shoreline run-up spectra?, *J. Geophys. Res.*, 82, 2577– 2581.

Iribarren, C. R., and C. Nogales (1949), Protection des Ports, paper presented at XVIIth International Navigation Congress, Lisbon, Portugal.

Kobayashi, N., G. S. DeSilva, and K. D. Watson (1989), Wave transformation and swash oscillation on gentle and steep slopes, *J. Geophys. Res.*, 94, 951– 966.

Lippmann, T. C., and R. A. Holman (1989), Quantification of sandbar morphology: A video technique based on wave dissipation, *J. Geophys. Res.*, 94, 995– 1011.

Longuet-Higgins, M. S., and R. W. Stewart (1962), Radiation stress and mass transport in gravity waves, with application to surfbeats, *J. Fluid Mech.*, 13, 481– 504.

Meyer, R. E., and A. D. Taylor (1972), Run-up on beaches, in *Waves on Beaches and Resulting Sediment Transport*, edited by R. E. Meyer, pp. 357– 411, Academic, San Diego, Calif.

Miche, R. (1951), Le Pouvoir reflechissant des ouvrages maritimes exposes a l'action de la houle, Ann. Ponts Chaussees, 121, 285– 319.

Osborne, P. D., and G. A. Rooker (1999), Sand re-suspension events in a high energy infragravity swash zone, J. Coastal. Res., 15, 74–86.

Pawka, S. (1982), Wave directional characteristics on a partially sheltered coast, Ph.D. thesis, Scripps Inst. of Oceanogr, Univ. of Calif., San Diego.

Plant, N. G., and R. A. Holman (1997), Intertidal beach profile estimation using video images, Mar. Geol., 140, 1 – 24.

Raubenheimer, B., and R. T. Guza (1996), Observations and predictions of run-up, J. Geophys. Res., 101, 25,575– 25,587.

Raubenheimer, B., R. T. Guza, S. Elgar, and N. Kobayashi (1995), Swash on a gently sloping beach, J. Geophys. Res., 100, 8751– 8760.

Ruessink, B. K., M. G. Kleinhan, and P. G. L. van den Beukel (1998), Observations of swash under highly dissipative conditions, J. Geophys. Res., 103, 3111– 3118.

Ruggiero, P., P. D. Komar, W. G. McDougal, and R. A. Beach (1996), Extreme water levels, wave runup and coastal erosion, paper presented at the 25th International Conference on Coastal Engineering, Am. Soc. of Civ. Eng., Orlando, Fla.

Ruggiero, P., P. D. Komar, J. J. Marra, W. G. McDougal, and R. A. Beach (2001), Wave runup, extreme water levels and the erosion of properties

backing beaches, J. Coastal Res., 17, 407–419.

Sallenger, A. H. (2000), Storm impact scale for barrier islands, J. Coastal Res., 16, 890–895.

Stoker, J. J. (1947), Surface waves in water of variable depth, Q. Appl. Math., 5(1), 1– 54.

Tillotsen, K. J., and P. D. Komar (1997), The wave climate of the Pacific Northwest (Oregon and Washington): A comparison of data sources,

J. Coastal Res., 13, 440– 452.

van der Meer, J. W., and C. J. Stam (1992), Wave runup on smooth and rock slopes of coastal structures, J. Waterw. Port Coastal Ocean Eng., 118, 534– 550.

R. A. Beach, Consortium for Oceanographic Research and Education,

1755 Massachusetts Avenue, NW, Suite 800, Washington, DC 20036-2102, USA.

R. A. Holman, College of Oceanic and Atmospheric Sciences, Oregon

State University, Corvallis, OR 97331, USA.

P. Ruggiero, Coastal and Marine Geology Program, U.S. Geological

Survey, 345 Middlefield Road, MS-999, Menlo Park, CA 94025, USA.

(pruggiero@usgs.gov)

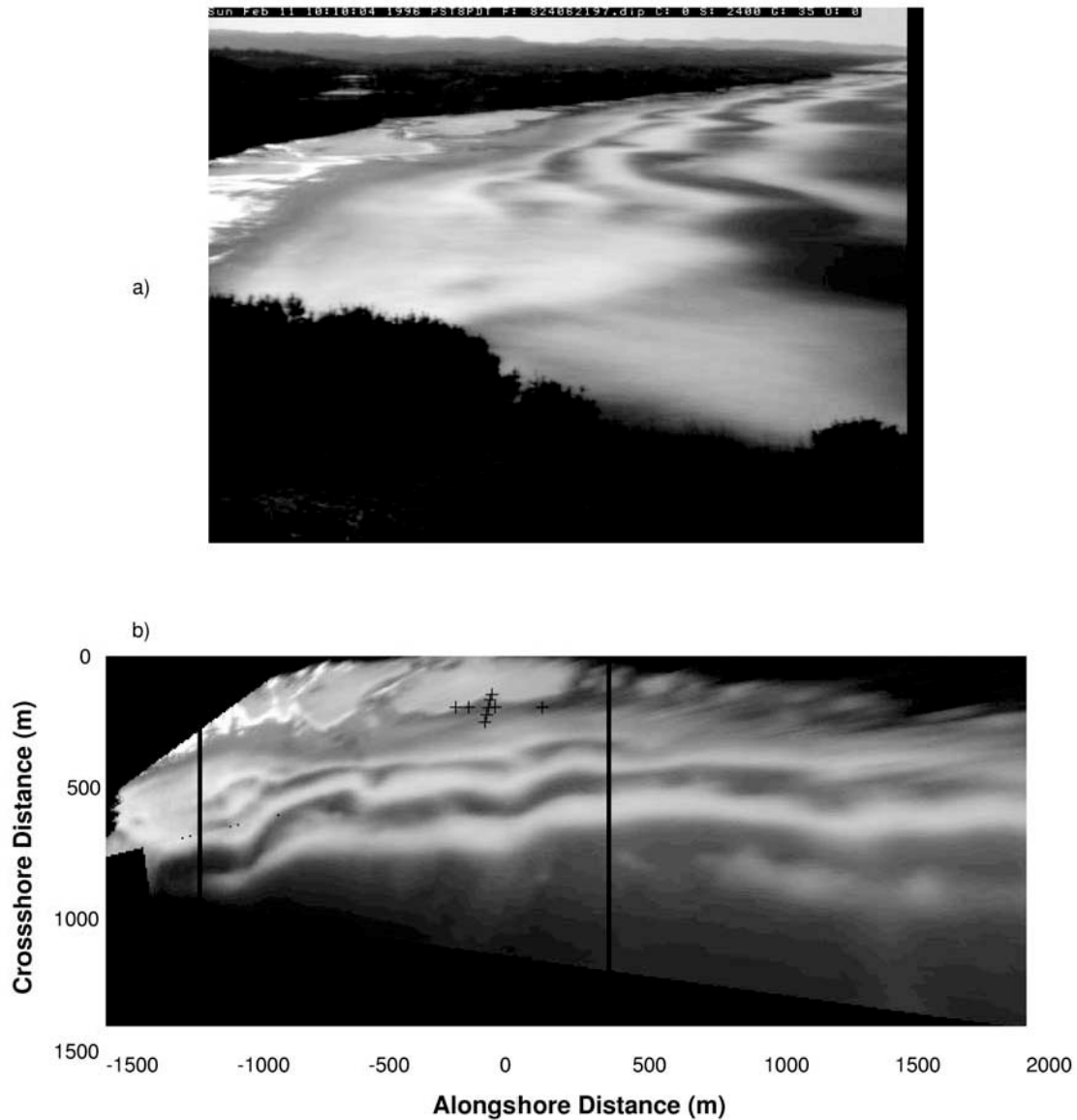


Figure 1. (a) Oblique and (b) plan view images from 10-min time-averaged Argus video exposures of Agate Beach, Oregon, on 11 February 1996, at low tide. Pluses in the plan view indicate the locations of in situ instrumentation during the experiment, and the solid lines indicate the alongshore extent of the run-up array.



Figure 2. “Snapshot” video image taken from northernmost facing run-up camera at 1600 LT on 11 February 1996. Solid lines indicate the locations of cross-shore transects 1– 7, spaced 50 m in the alongshore, over which run-up was digitized.

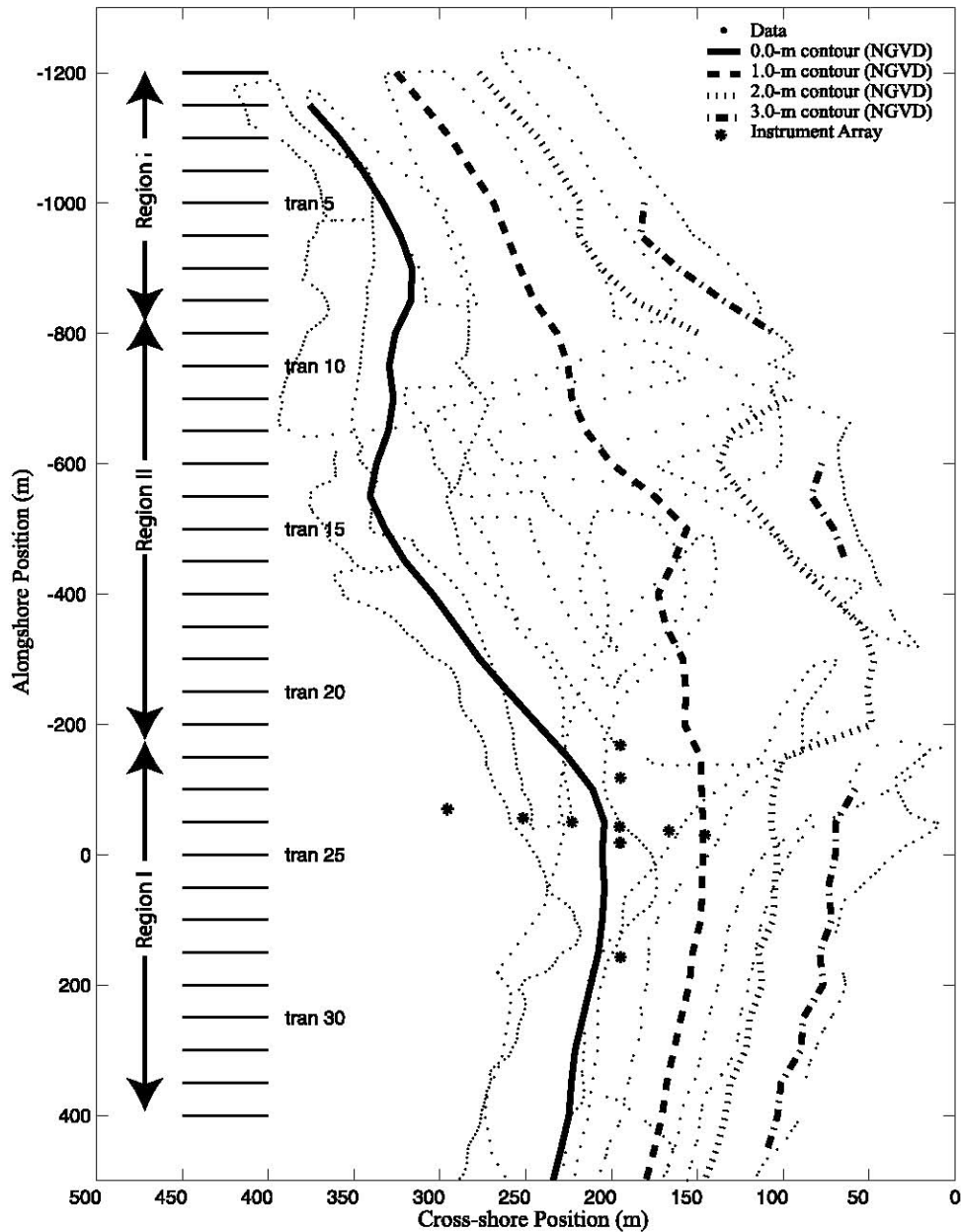


Figure 3. Topographic contour map of Agate Beach, Oregon, surveyed on 11 February 1996. The dots correspond to the individual survey measurements, and the various lines reveal the elevation contours referenced to the U.S. National Geodetic Vertical Datum (NGVD) of 1929. The asterisks indicate the locations of the in situ instrumentation, and the solid lines perpendicular to the contours show the alongshore locations of the 33 transects along which run-up time series were extracted and analyzed.

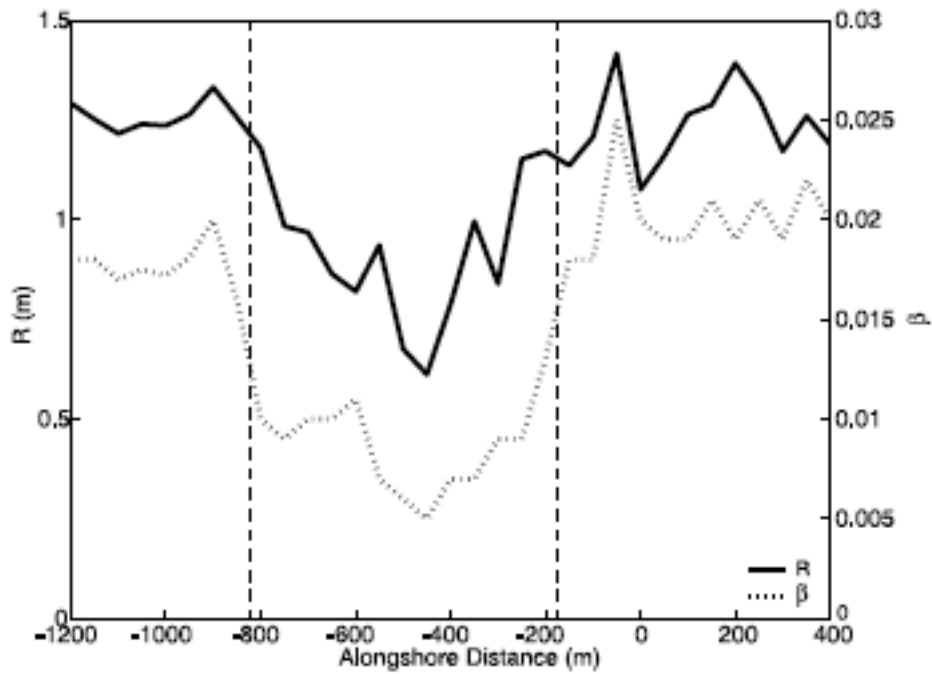


Figure 4. Significant vertical run-up elevation (solid line) and foreshore beach slope (dashed line) as a function of alongshore position for the 11 February 1996, Agate Beach data run. The dashed vertical lines separate the lower sloping region II from region I.

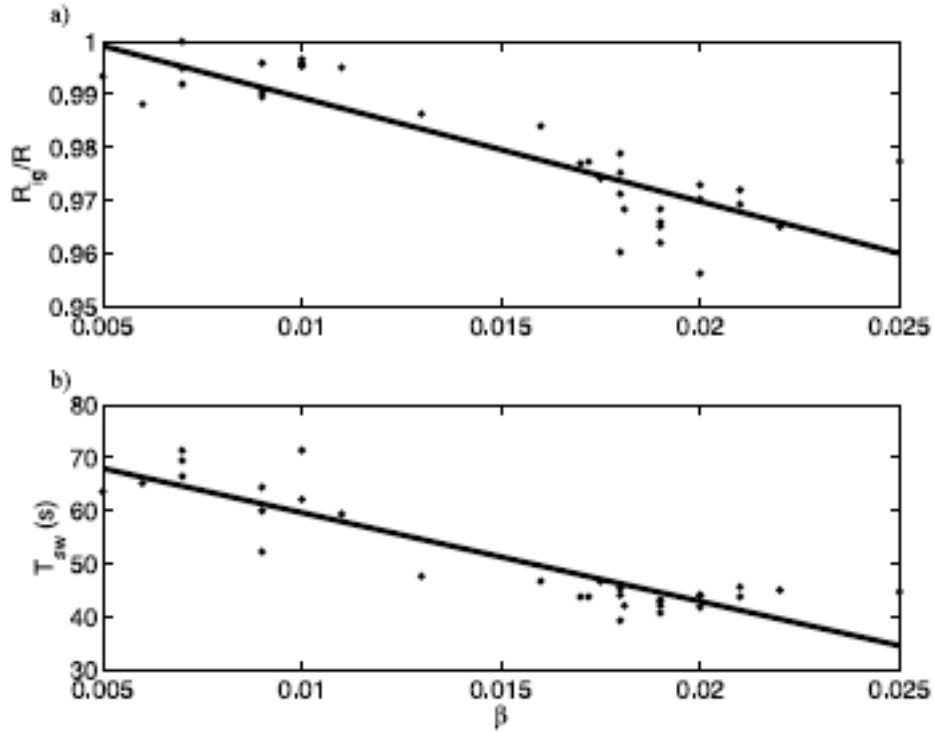


Figure 5. (a) The ratio R_{ig}/R and (b) the significant run-up period, T_{sw} , versus foreshore beach slope, β . Best fit lines are $R_{ig}/R = -1.9\beta + 1.0$, $r = -0.86$ and $T_{sw} = -1.7 \times 10^3\beta + 76.4$, $r = -0.90$.

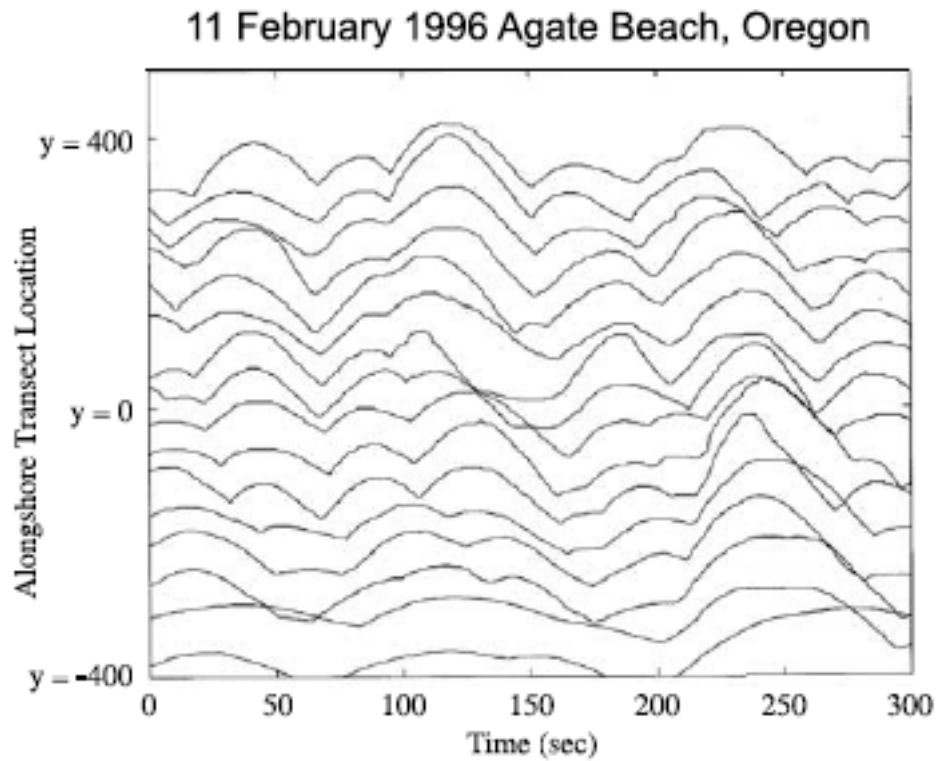


Figure 6. Typical 5-min run-up time series from the 11 February 1996, 1559 LT data run from the Agate Beach experiment. Cross-shore transects at which run-up was measured are offset vertically, spaced at 50 m.

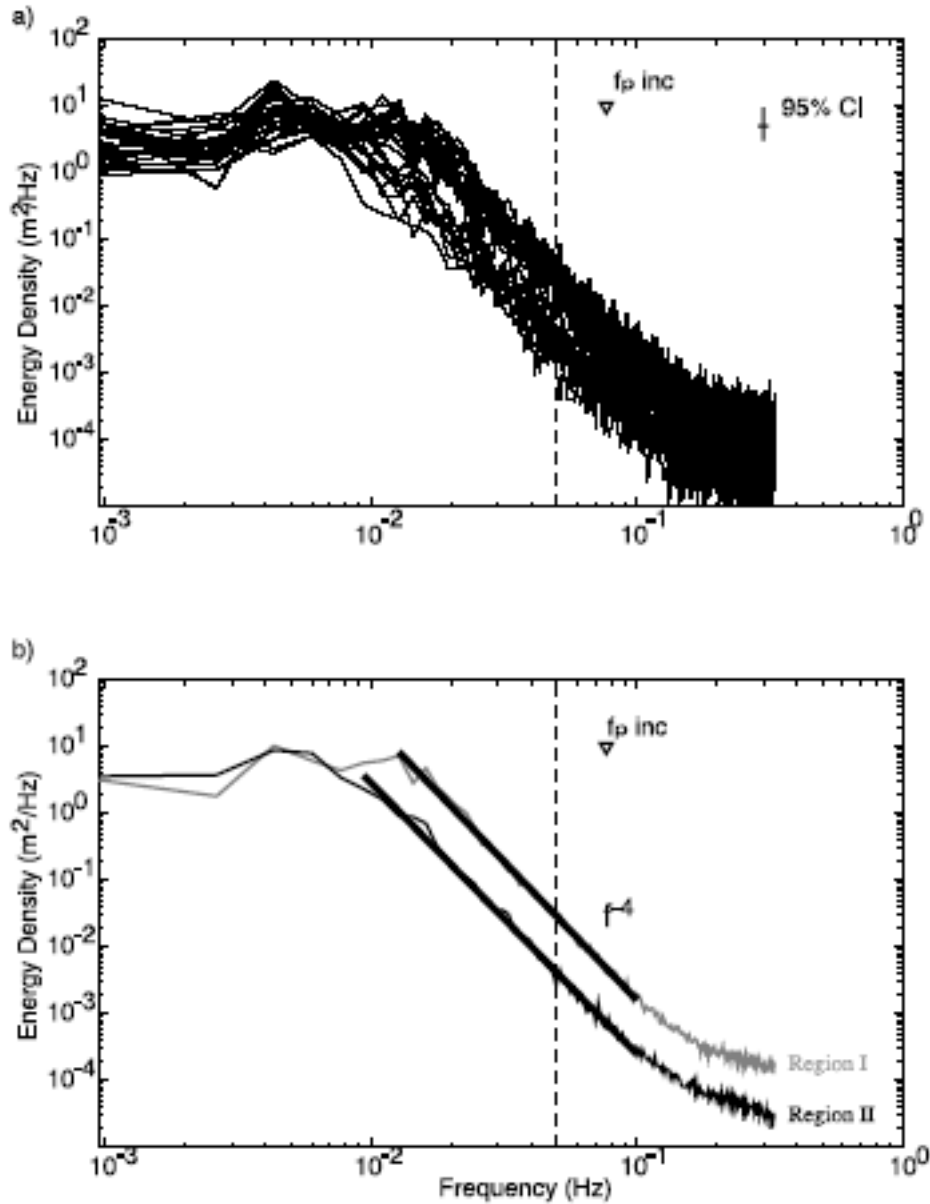


Figure 7. (a) Observed run-up energy density spectra from all 33 transects and (b) average energy density spectra from region I (top shaded line) and from region II (bottom solid line). The triangles indicate the peak frequency of the deep water waves, and the vertical dashed lines at 0.05 Hz indicate the division between the infragravity and the sea swell frequency bands. The solid lines through the spectra within the saturated band are the best fits to the estimates in log-log space. The line in region I has the form $E(f) = 1.2 \times 10^{-7} f^{4.1}$, while in region II, $E(f) = 2.2 \times 10^{-8} f^{4.0}$.

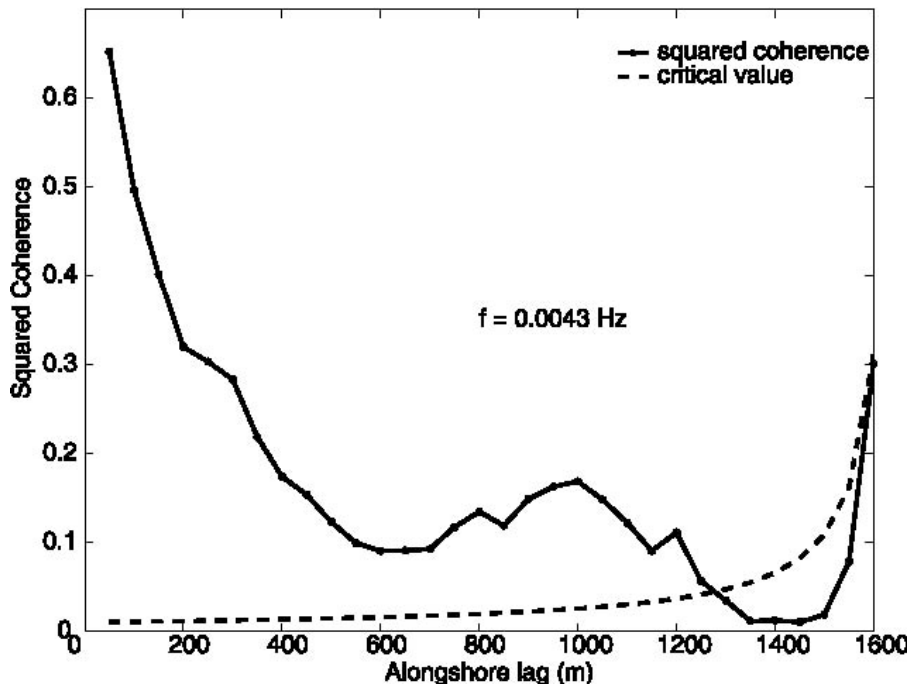


Figure 8. Squared coherence (solid line) and the 95% significance level (dashed line) versus alongshore lag for the peak frequency, $f = 0.0043 \text{ Hz}$, of the average energy density spectrum in region I.

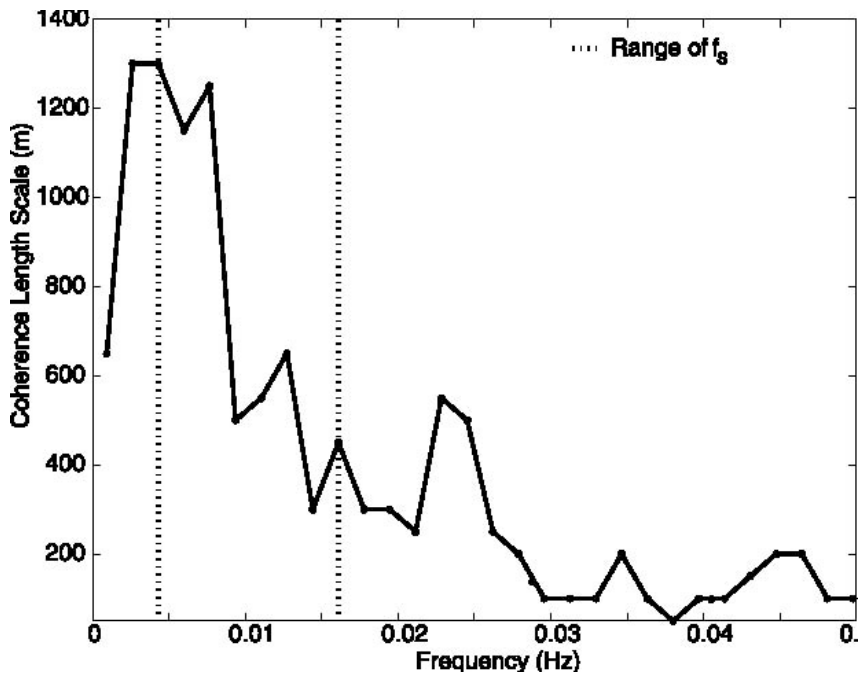


Figure 9. Alongshore coherence length scale, L_c , within

the infragravity band as a function of frequency. The dotted vertical lines indicate the range of lowest saturated frequencies, f_s , during the 11 February 1996, Agate Beach data run.

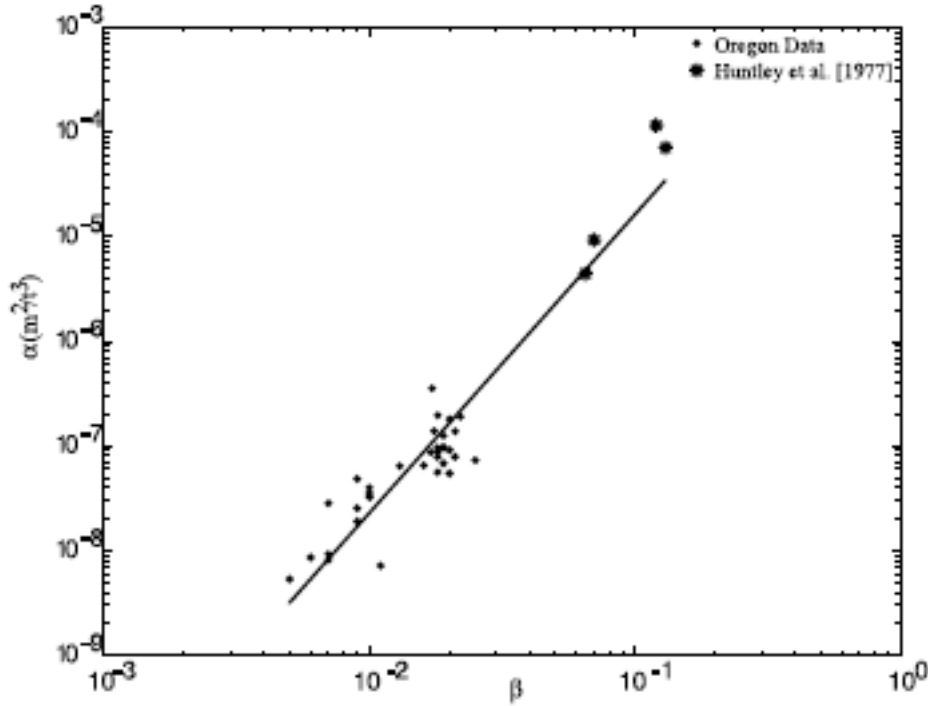


Figure 10. Dimensional constant α estimated from the saturated region of run-up energy density spectra as a function of foreshore beach slope. Closed circles are from the 11 February 1996, Agate Beach data run while the asterisks circles are taken from Huntley et al. [1977]. The solid line is the best fit through both data sets in log-log space.

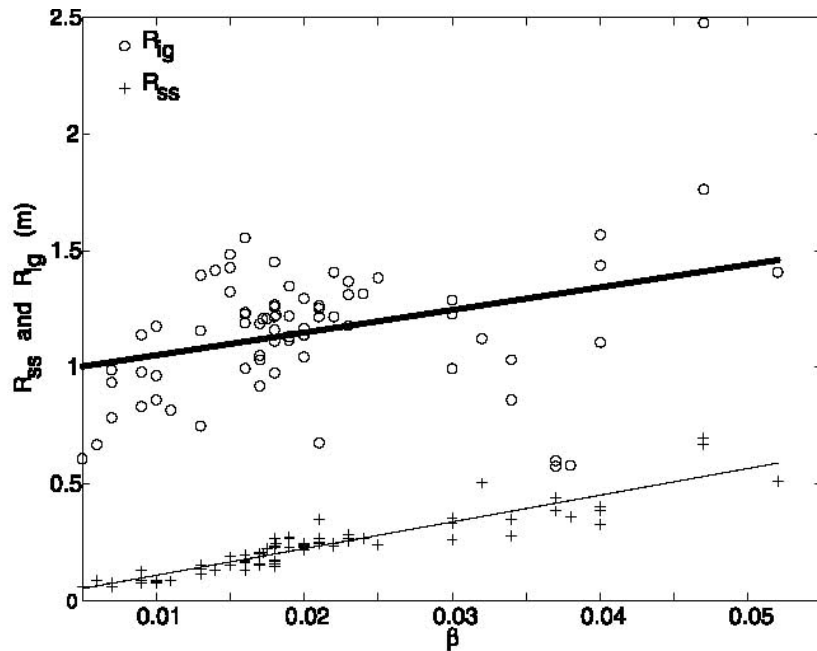


Figure 11. Infragravity band significant run-up, R_{ig} (circles), and sea swell significant run-up, R_{ss} (pluses) versus beach slope for all of the Oregon run-up data. Best fit lines are $R_{ig} = 9.7 \beta + 1.0$, $r = 0.34$ (heavy solid line) and $R_{ss} = 11.4 \beta - 0.01$, $r = 0.92$ (light solid line).

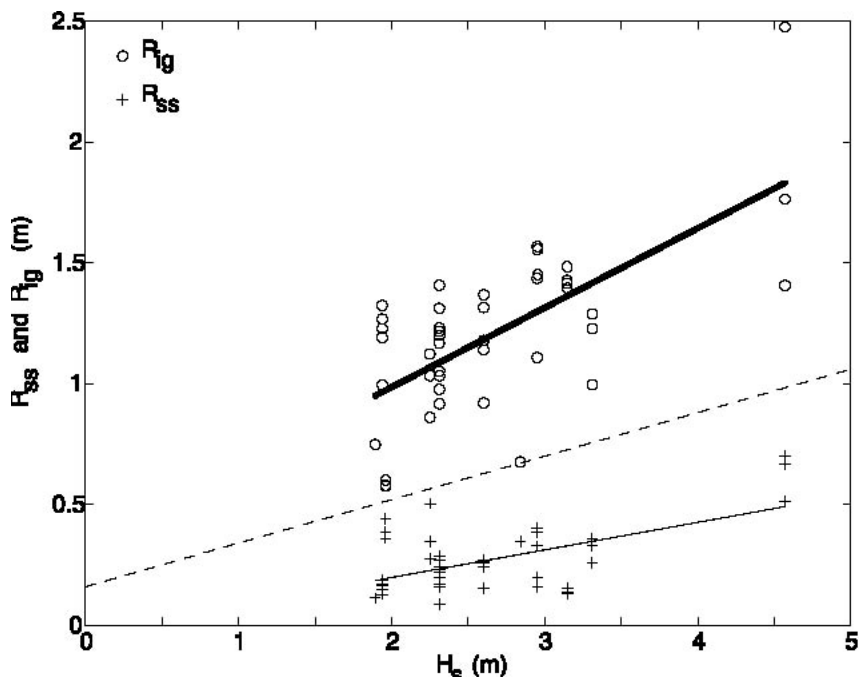


Figure 12. Band separated vertical run-up elevation versus deep water significant wave height for all Oregon

data. Circles represent low frequencies ($R_{ig}, f < 0.05$ Hz) and pluses indicate high frequencies ($R_{ss}, f > 0.05$ Hz). The solid lines are the best fit through the Oregon data; $R_{ig} = 0.33 H_s + 0.33$, $r = 0.67$ (heavy solid line) and $R_{ss} = 0.11 H_s - 0.03$, $r = 0.56$ (light solid line), and the dashed line is the relationship from Ruessink et al. [1998], $R_{ig} = 0.18 H_s + 0.16$.

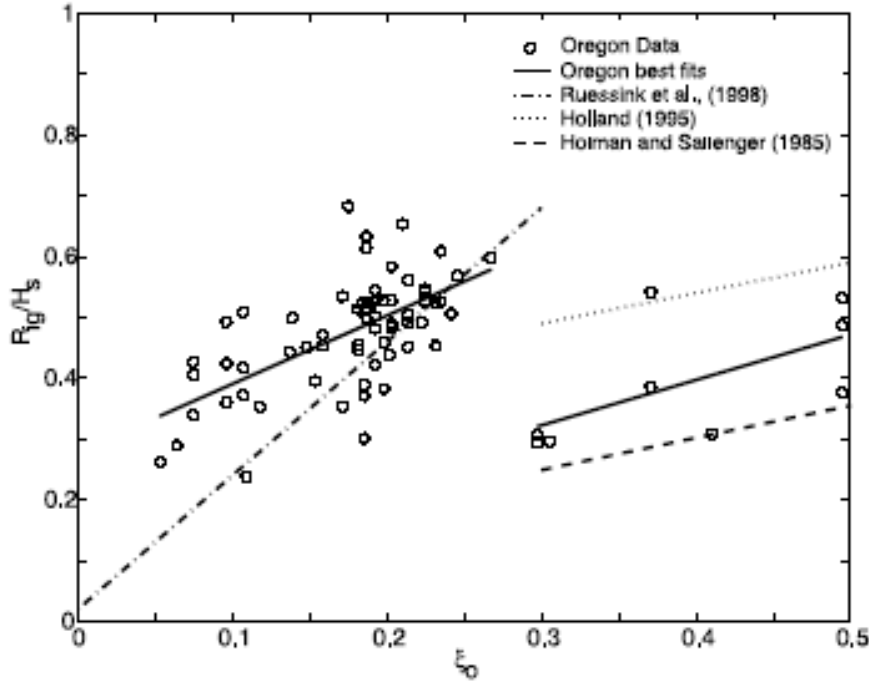


Figure 13. Normalized significant infragravity run-up elevation versus Iribarren number. The circles represent all of the Oregon run-up data and the solid lines are the linear relationships for $\xi_o < 0.3$, $R_{ig}/H_s = 1.12 \xi_o + 0.28$, $r = 0.62$ and for $\xi_o > 0.3$, $R_{ig}/H_s = 0.75 \xi_o + 0.01$, $r = 0.62$. Also shown are the relationships of Ruessink et al. [1998], $R_{ig}/H_s = 2.20 \xi_o + 0.02$ (dash-dotted line), Holland [1995], $R_{ig}/H_s = 0.5 \xi_o + 0.34$ (dotted line), and Holman and Sallenger [1985], $R_{ig}/H_s = 0.53 \xi_o + 0.09$ (dashed line).